

Figure 1: Surface temperatures in the Sargasso Sea, a 2 million square mile region of the Atlantic Ocean, with time resolution of 50 to 100 years and ending in 1975, as determined by isotope ratios of marine organism remains in sediment at the bottom of the sea (3). The horizontal line is the average temperature for this 3,000-year period. The Little Ice Age and Medieval Climate Optimum were naturally occurring, extended intervals of climate departures from the mean. A value of 0.25 °C, which is the change in Sargasso Sea temperature between 1975 and 2006, has been added to the 1975 data in order to provide a 2006 temperature value.

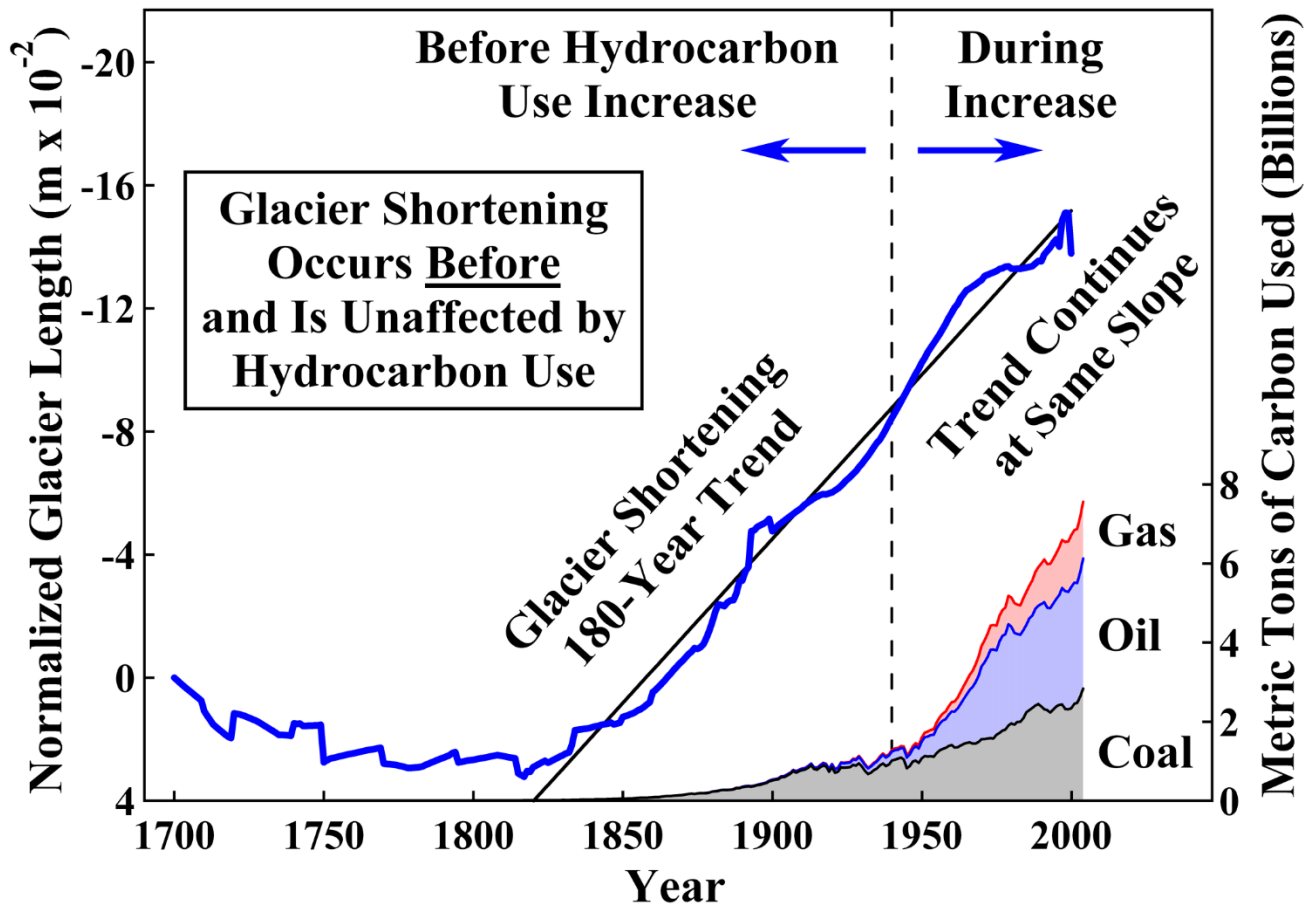


Figure 2: Average length of 169 glaciers from 1700 to 2000 (4). The principal source of melt energy is solar radiation. Variations in glacier mass and length are primarily due to temperature and precipitation (5,6). This melting trend lags the temperature increase by about 20 years, so it pre dates the 6-fold increase in hydrocarbon use (7) even more than shown in the figure. Hydrocarbon use could not have caused this shortening trend.

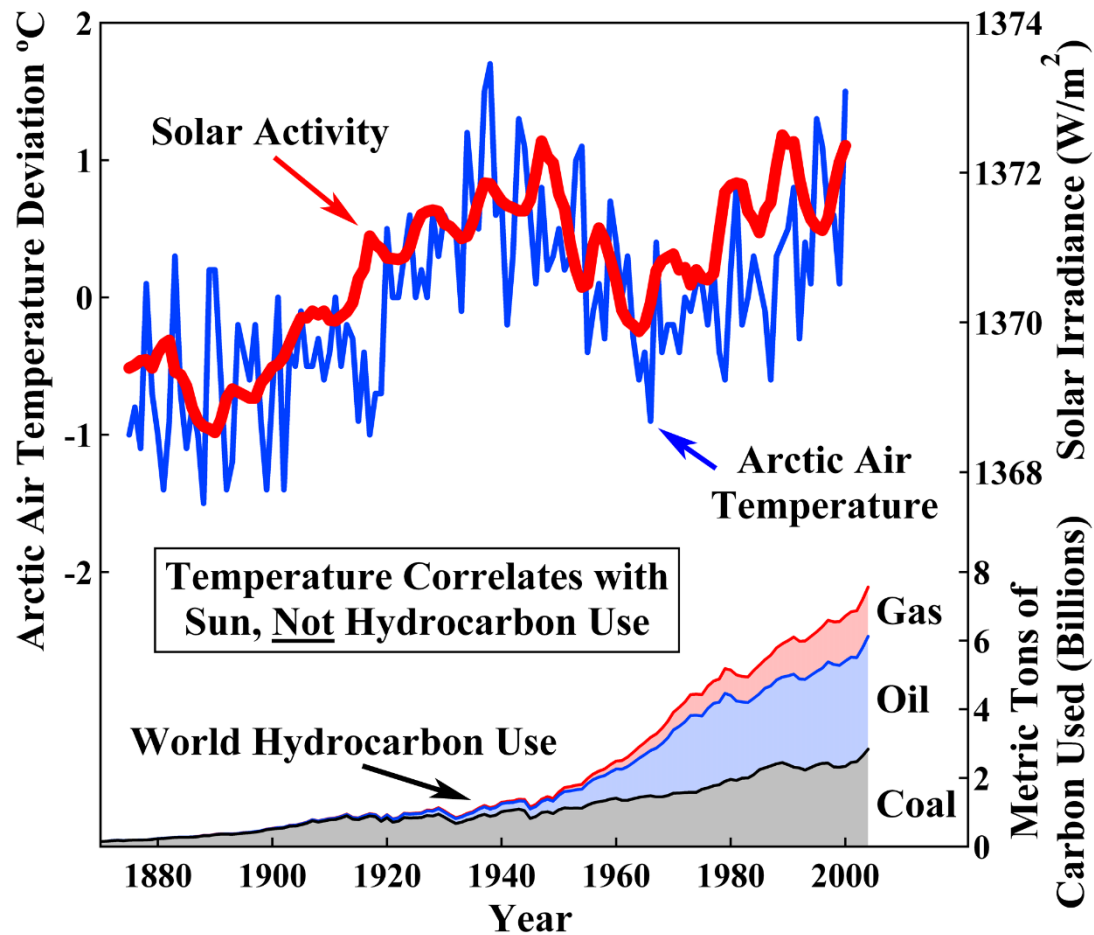


Figure 3: Arctic surface air temperature compared with total solar irradiance as measured by sunspot cycle amplitude, sunspot cycle length, solar equatorial rotation rate, fraction of penumbral spots, and decay rate of the 11-year sunspot cycle (8,9). Solar irradiance correlates well with Arctic temperature, while hydrocarbon use (7) does not correlate.

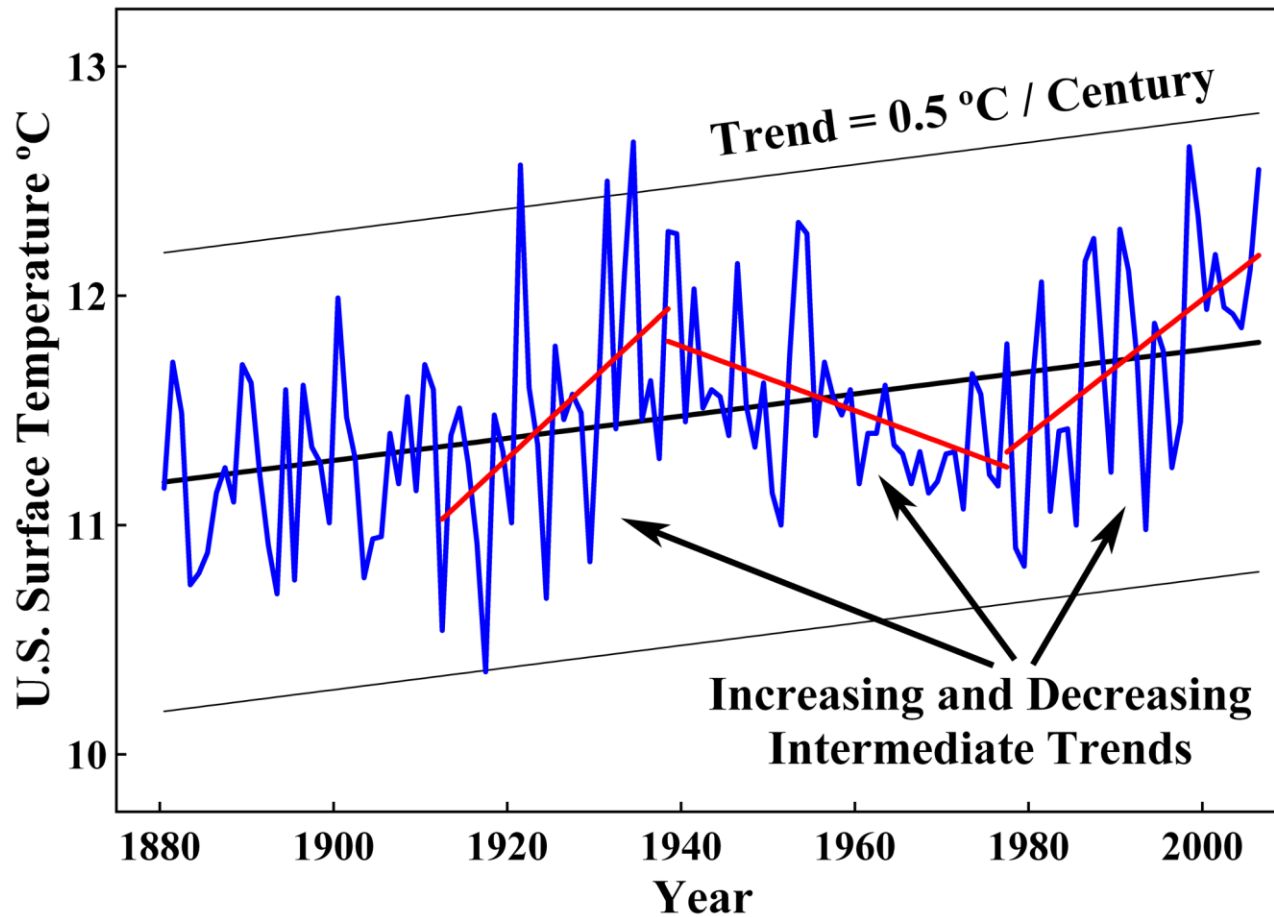


Figure 4: Annual mean surface temperatures in the contiguous United States between 1880 and 2006 (10). The slope of the least-squares trend line for this 127-year record is 0.5 °C per century.

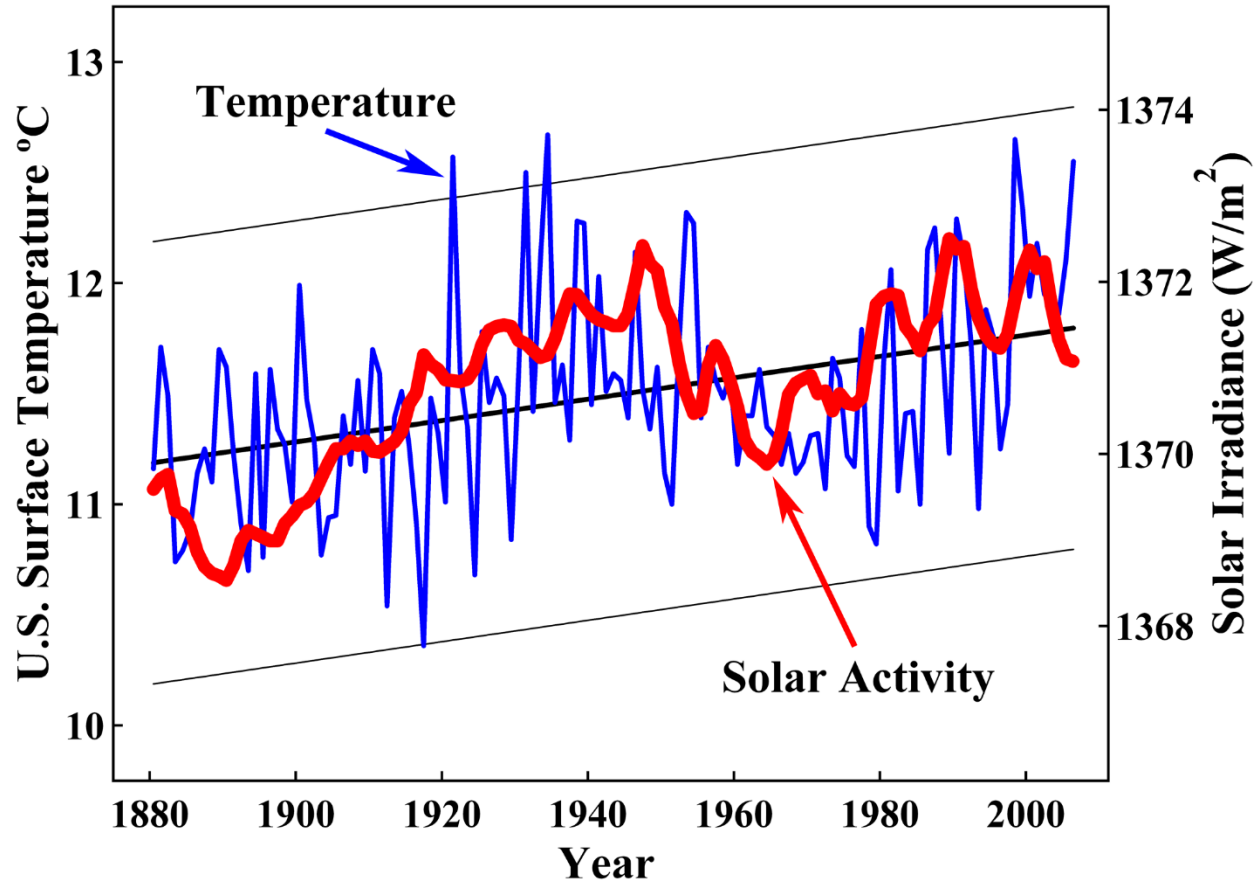


Figure 5: U.S. surface temperature from Figure 4 as compared with total solar irradiance (19) from Figure 3.

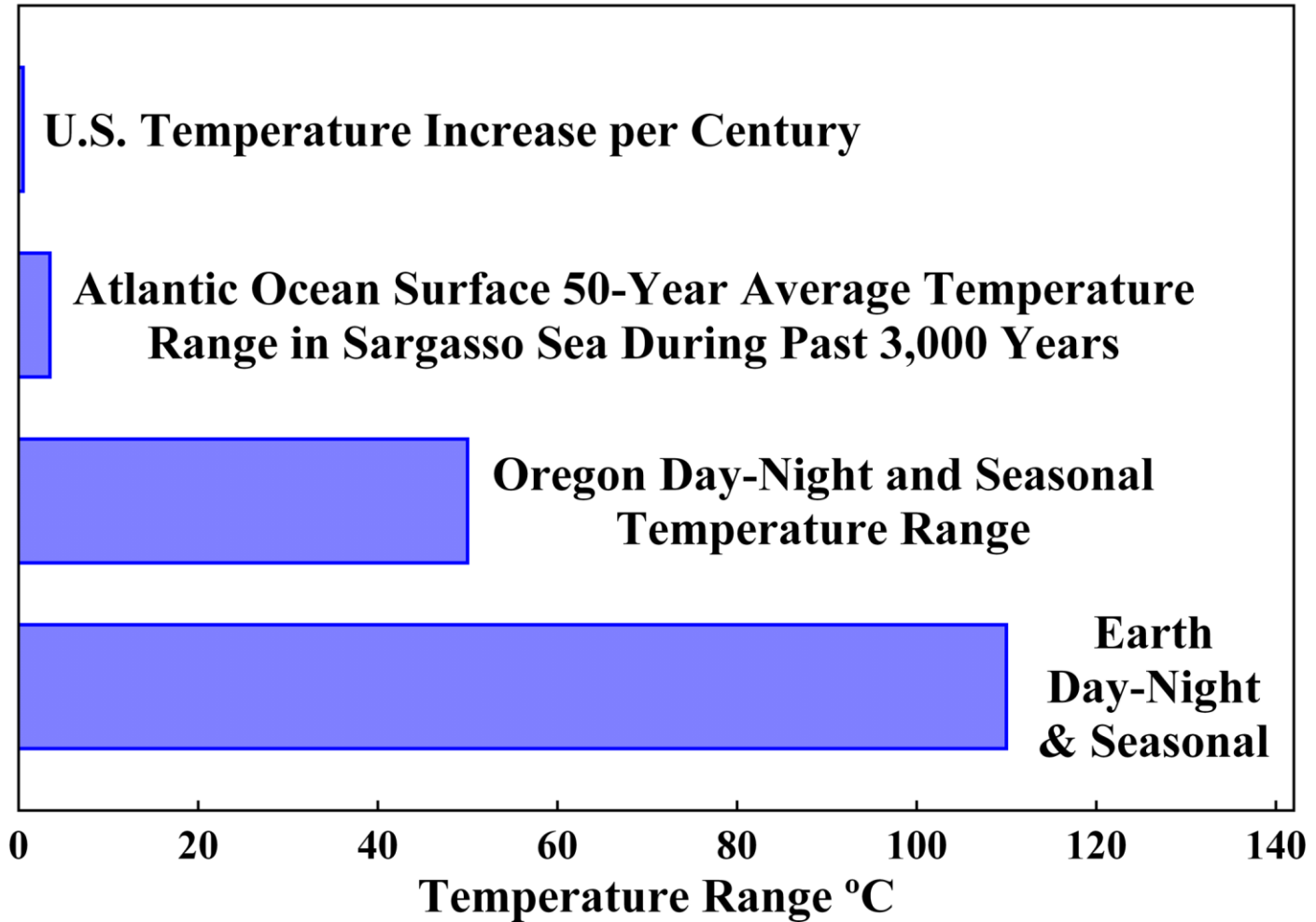


Figure 6: Comparison between the current U.S. temperature change per century, the 3,000-year temperature range in Figure 1, seasonal and diurnal range in Oregon, and seasonal and diurnal range throughout the Earth.

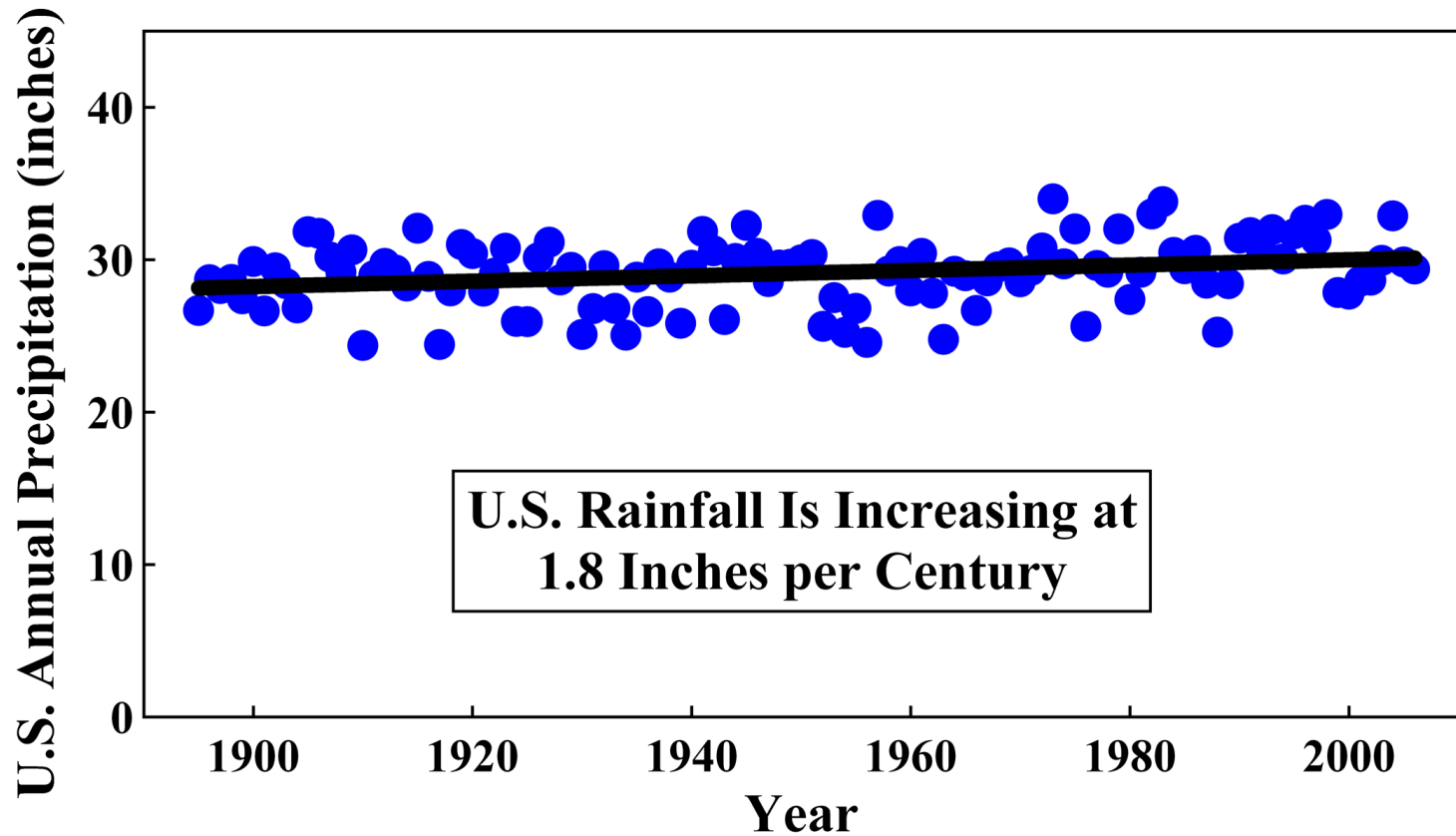


Figure 7: Annual precipitation in the contiguous 48 United States between 1895 and 2006. U.S. National Climatic Data Center, U.S. Department of Commerce 2006 Climate Review (20). The trend shows an increase in rainfall of 1.8 inches per century approximately 6% per century.

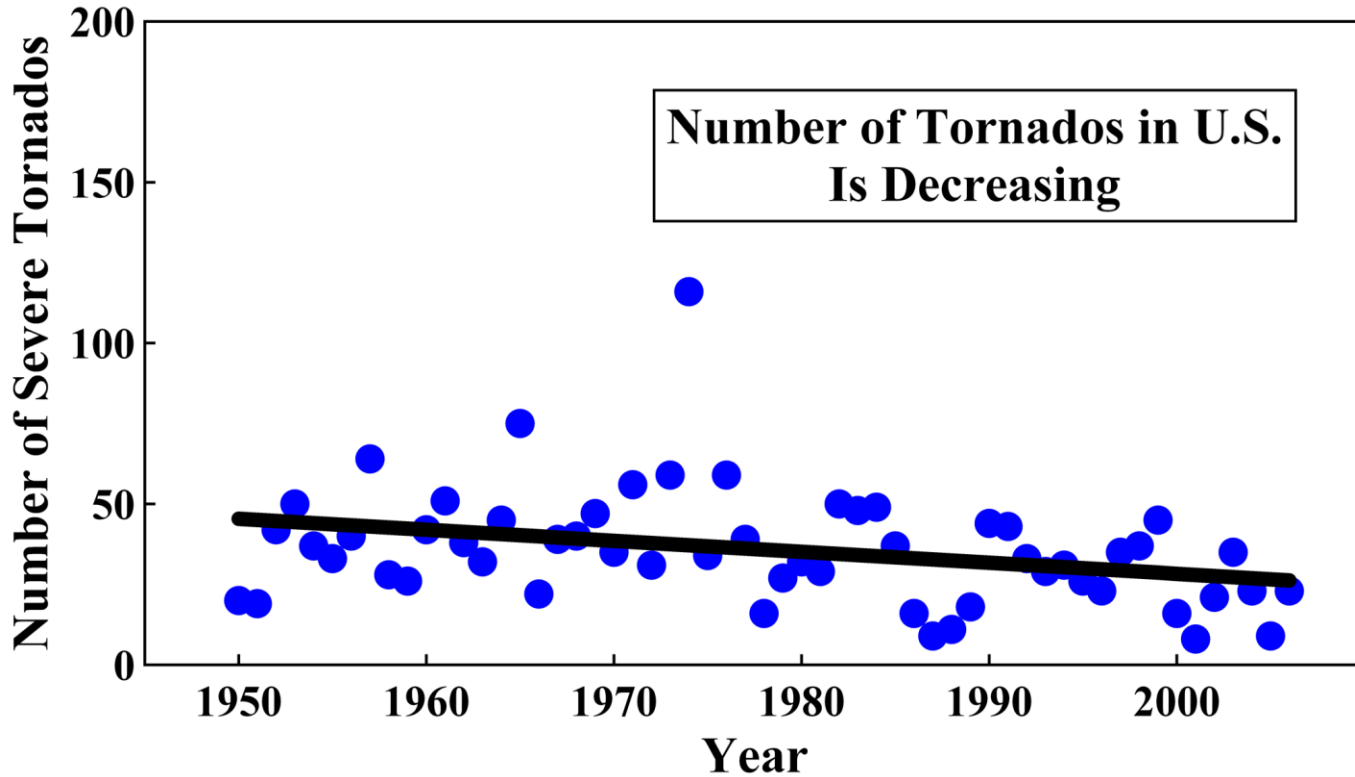


Figure 8: Annual number of strong-to-violent category F3 to F5 tornadoes during the March-to-August tornado season in the U.S. between 1950 and 2006. U.S. National Climatic Data Center, U.S. Department of Commerce 2006 Climate Review (20). During this period, world hydrocarbon use increased 6-fold, while violent tornado frequency decreased by 43%.

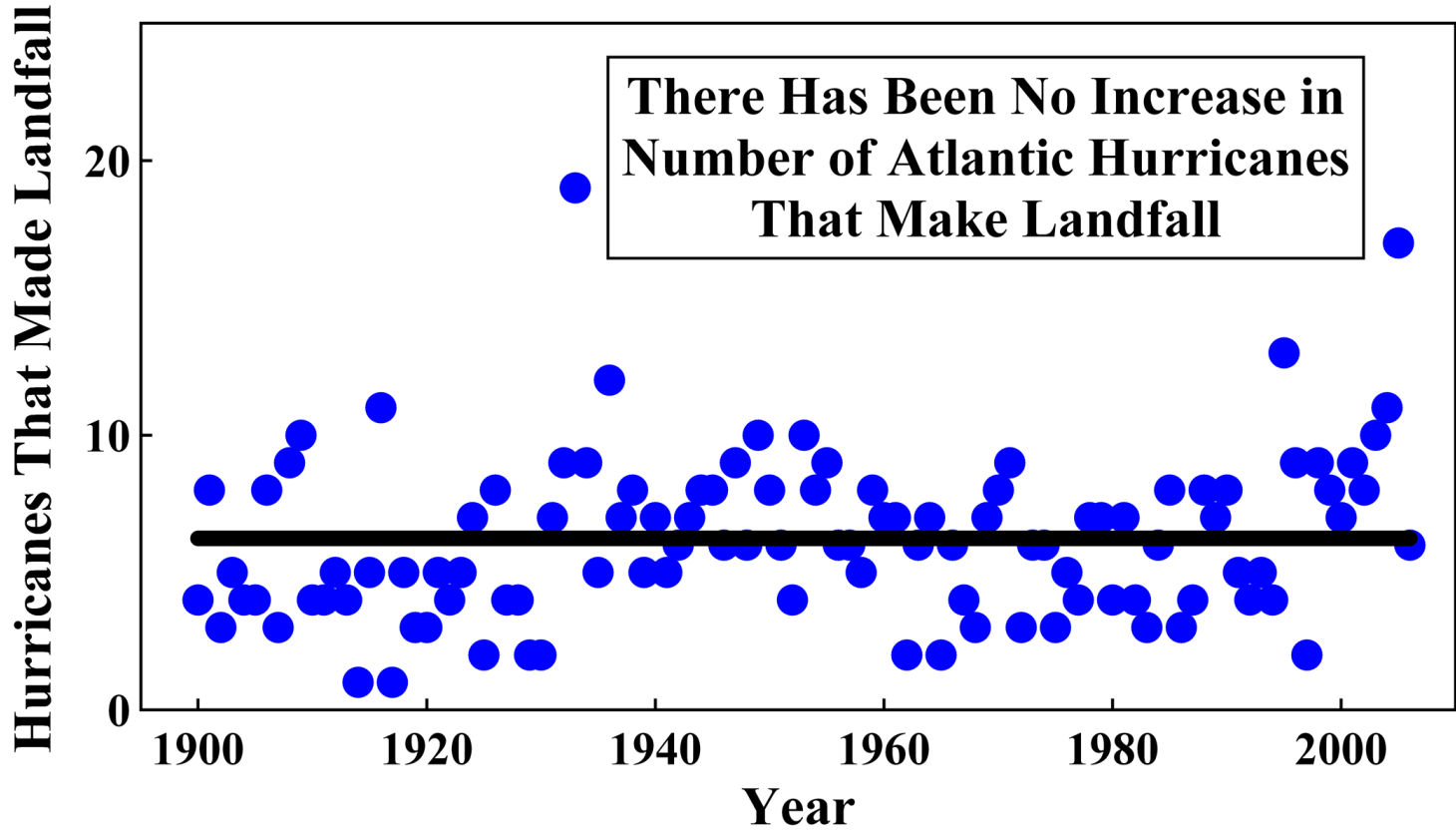


Figure 9: Annual number of Atlantic hurricanes that made land fall between 1900 and 2006 (21). Line is drawn at mean value.

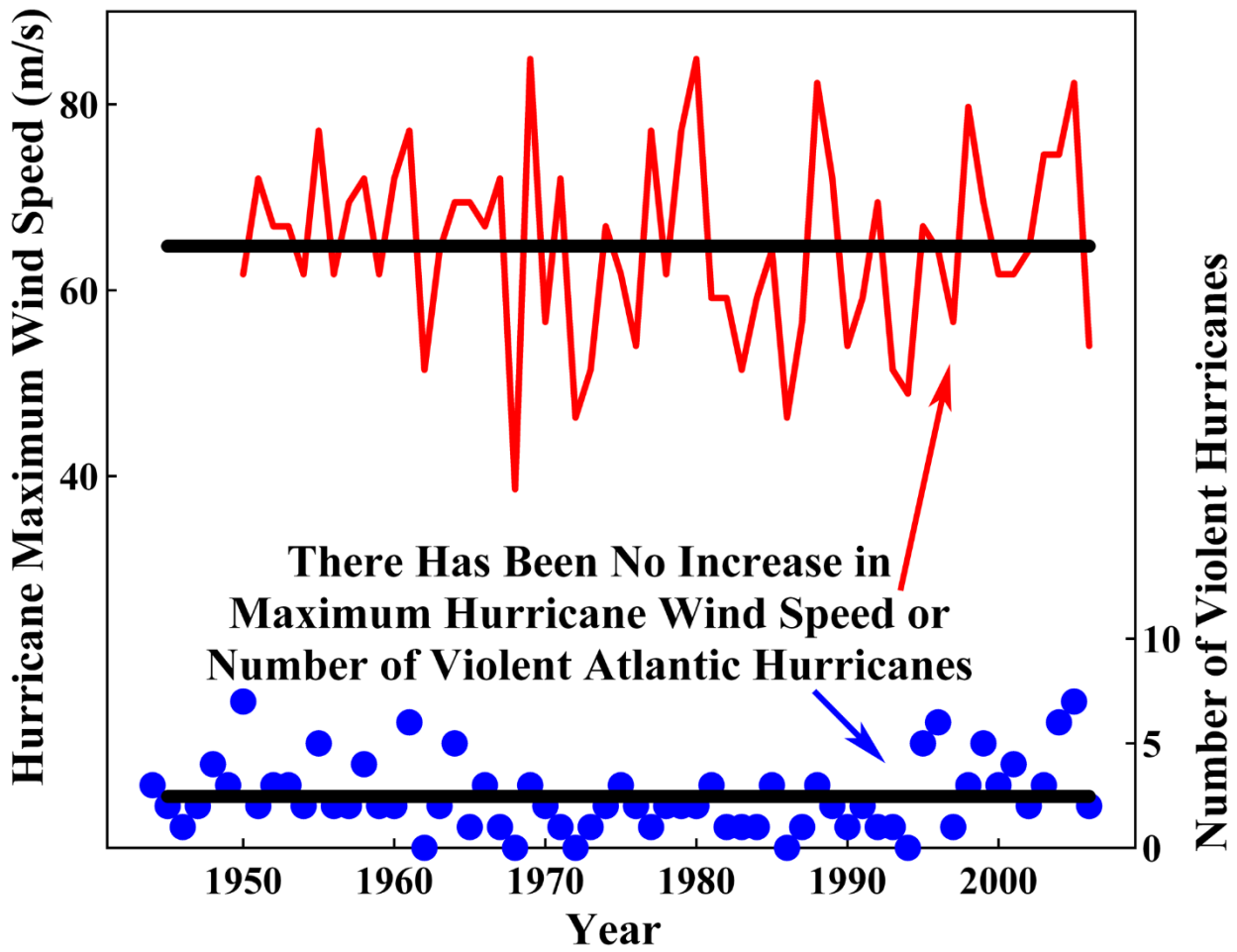


Figure 10: Annual number of violent hurricanes and maximum attained wind speed during those hurricanes in the Atlantic Ocean between 1944 and 2006 (22,23). There is no upward trend in either of these records. During this period, world hydrocarbon use increased 6-fold. Lines are mean values.

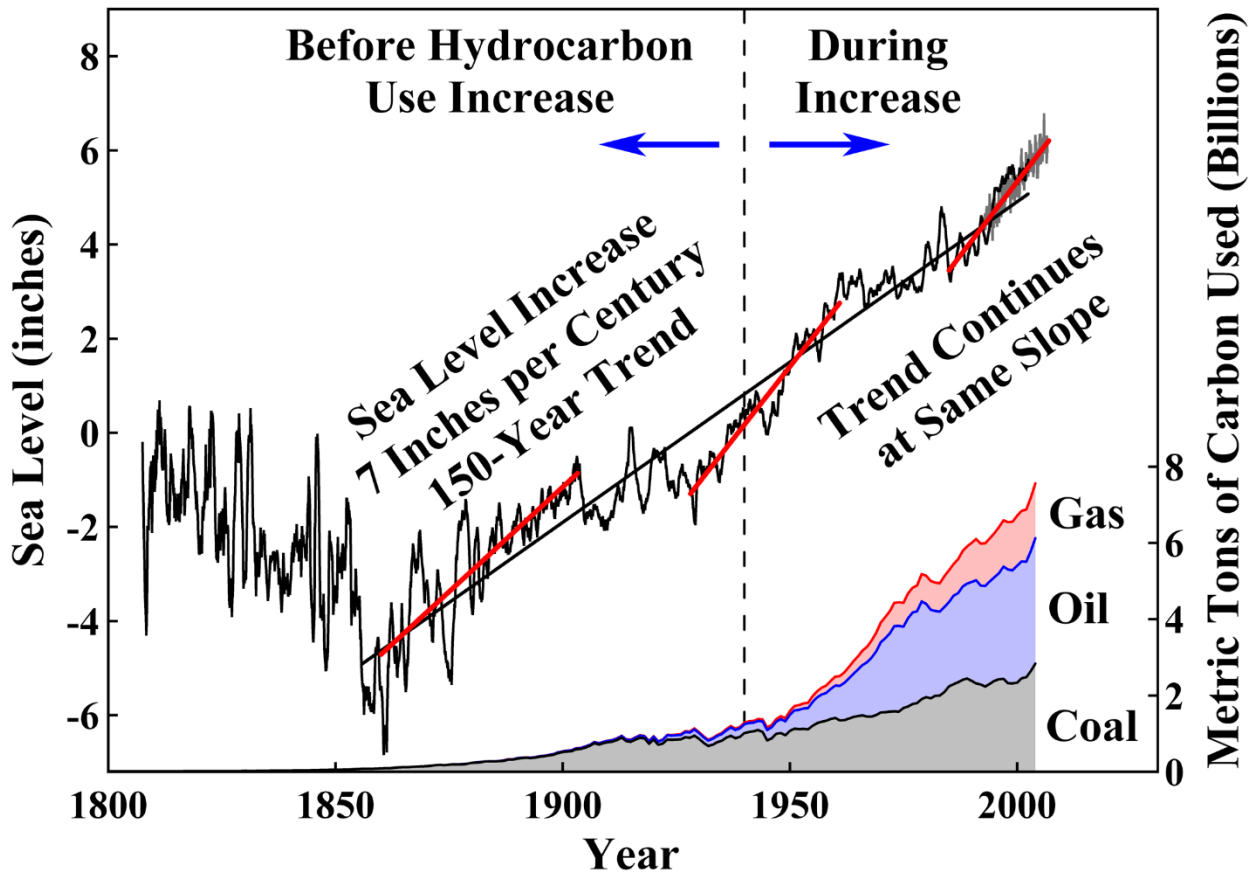


Figure 11: Global sea level measured by surface gauges between 1807 and 2002 (24) and by satellite between 1993 and 2006 (25). Satellite measurements are shown in gray and agree with tide gauge measurements. The overall trend is an increase of 7 inches per century. Intermediate trends are 9, 0, 12, 0, and 12 inches per century, respectively. This trend lags the temperature increase, so it predates the increase in hydrocarbon use even more than is shown. It is unaffected by the very large increase in hydrocarbon use.

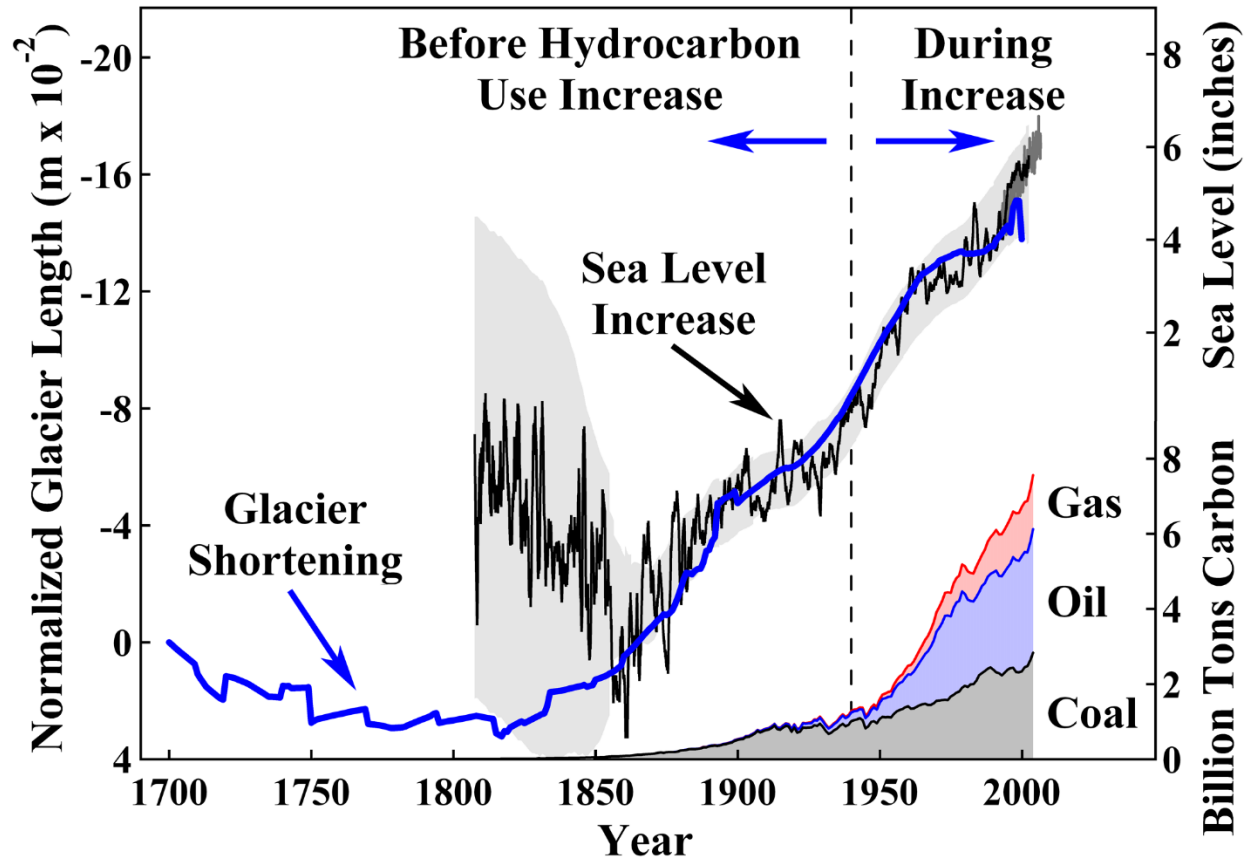


Figure 12: Glacier shortening (4) and sea level rise (24,25). Gray area designates estimated range of error in the sea level record. These measurements lag air temperature increases by about 20 years. So, the trends began more than a century before increases in hydrocarbon use.

<b>Table 1: Query</b>	<b>Yes</b>	<b>No</b>	<b>Yes/No</b>	<b>Two-Tailed Probability</b>
Warm Climatic Anomaly 800-1300 A.D.?	<b>88</b>	2	7	> 99.99
Cold Climatic Anomaly 1300-1900 A.D.?	<b>105</b>	2	2	> 99.99
20th Century Warmest in Individual Record?	7	<b>64</b>	14	< 0.0001

Table 1: Comprehensive review of all instances in which temperature or temperature-correlated records from localities throughout the world permit answers to queries concerning the existence of the Medieval Climate Optimum, the Little Ice Age, and an unusually warm anomaly in the 20th century (11). The compiled and tabulated answers confirm the three principal features of the Sargasso Sea record shown in Figure 1. The probability that the answer to the query in column 1 is yes is given in column 5.

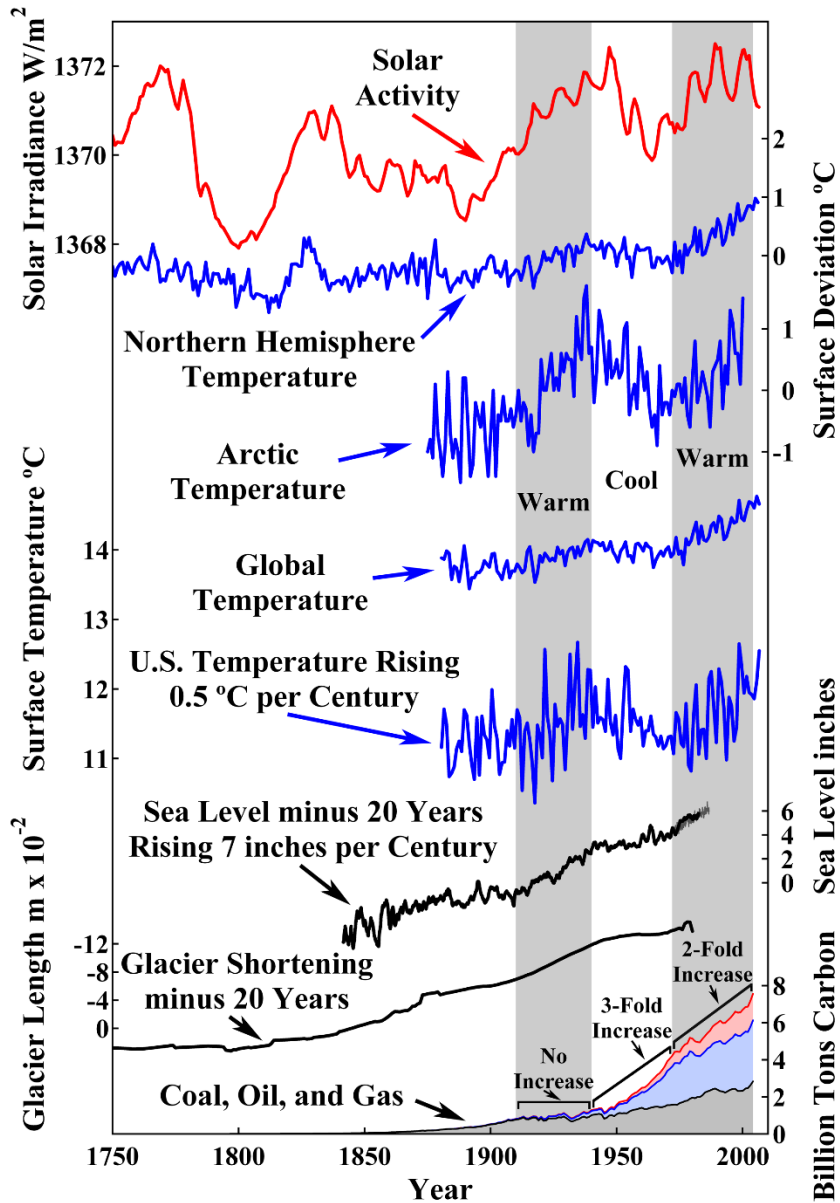


Figure 13: Seven independent records solar activity (9); Northern Hemisphere, (13), Arctic (28), global (10), and U.S. (10) annual surface air temperatures; sea level (24,25); and glacier length (4) all qualitatively confirm each other by exhibiting three intermediate trends warmer, cooler, and warmer. Sea level and glacier length are shown minus 20 years, correcting for their 20-year lag of atmospheric temperature. Solar activity, Northern Hemisphere temperature, and glacier lengths show a low in about 1800.

Hydrocarbon use (7) is uncorrelated with temperature. Temperature rose for a century before significant hydrocarbon use. Temperature rose between 1910 and 1940, while hydrocarbon use was almost unchanged. Temperature then fell between 1940 and 1972, while hydrocarbon use rose by 330%. Also, the 150 to 200-year slopes of the sea level and glacier trends were unchanged by the very large increase in hydrocarbon use after 1940.

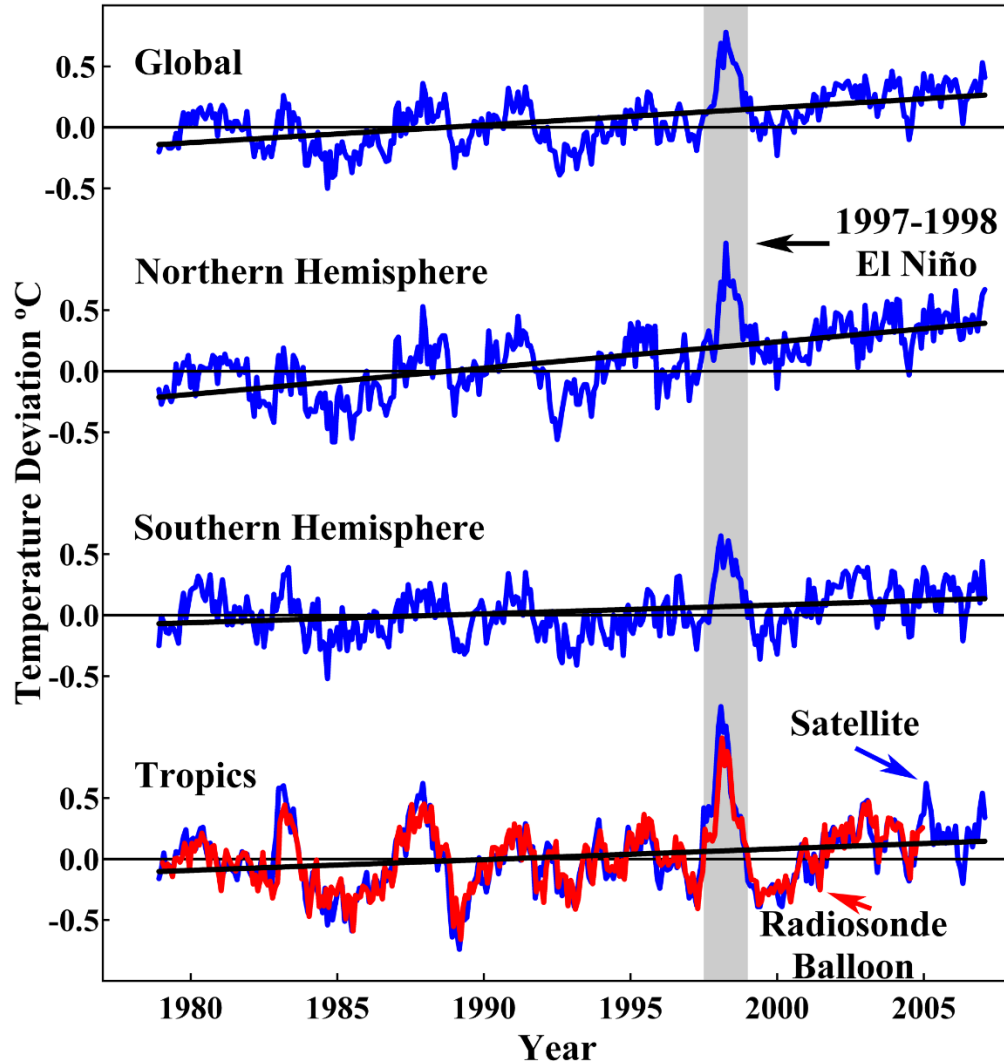


Figure 14: Satellite microwave sounding unit (blue) measurements of tropospheric temperatures in the Northern Hemisphere between 0 and 82.5 N, Southern Hemisphere between 0 and 82.5 S, tropics between 20S and 20N, and the globe between 82.5N and 82.5S between 1979 and 2007 (29), and radiosonde balloon (red) measurements in the tropics (29). The balloon measurements confirm the satellite technique (29-31). The warming anomaly in 1997-1998 (gray) was caused by El Niño, which, like the overall trends, is unrelated to CO<sub>2</sub> (32).

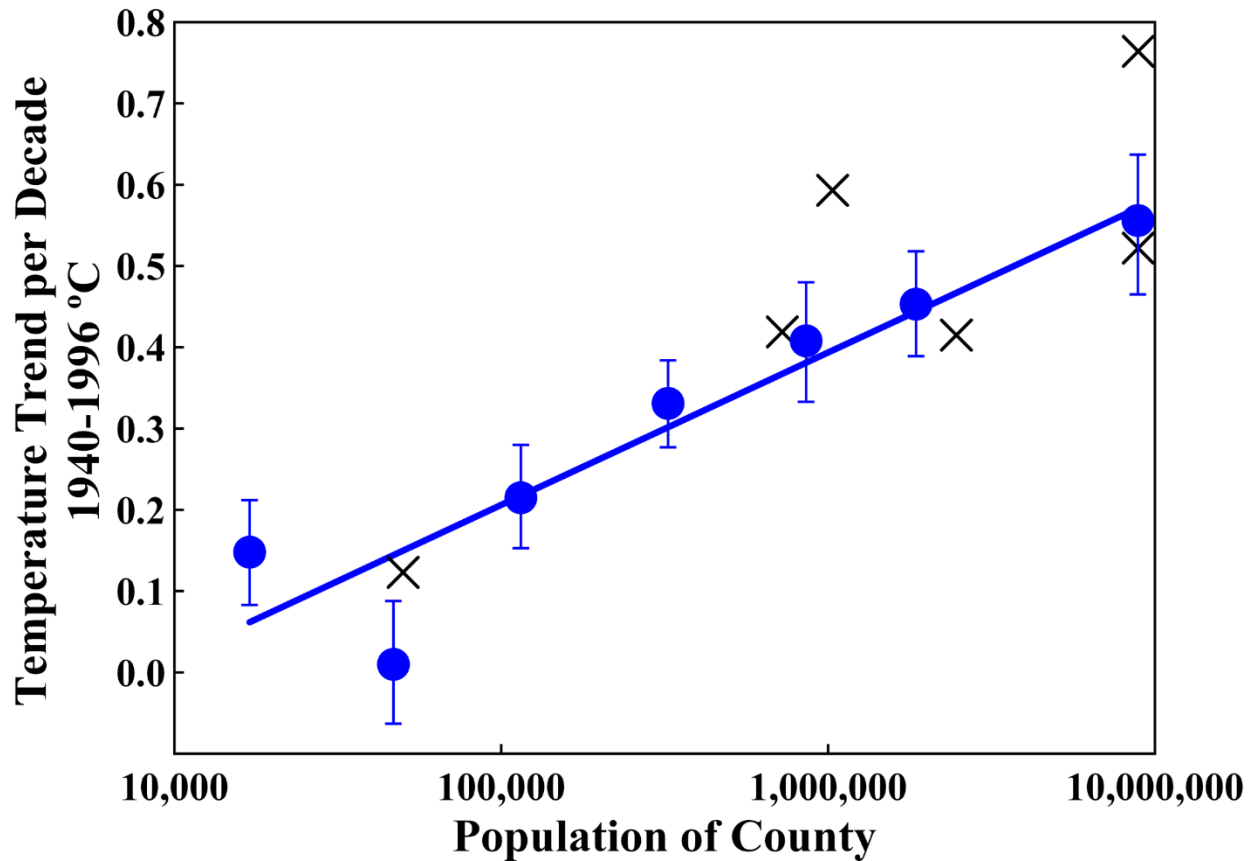


Figure 15: Surface temperature trends for 1940 to 1996 from 107 measuring stations in 49 California counties (51,52). The trends were combined for counties of similar population and plotted with the standard errors of their means. The six measuring stations in Los Angeles County were used to calculate the standard error of that county, which is plotted at a population of 8.9 million. The urban heat island effect on surface measurements is evident. The straight line is a least-squares fit to the closed circles. The points marked X are the six unadjusted station records selected by NASAGISS (53-55) for use in their estimate of global surface temperatures. Such selections make NASA GISS temperatures too high.

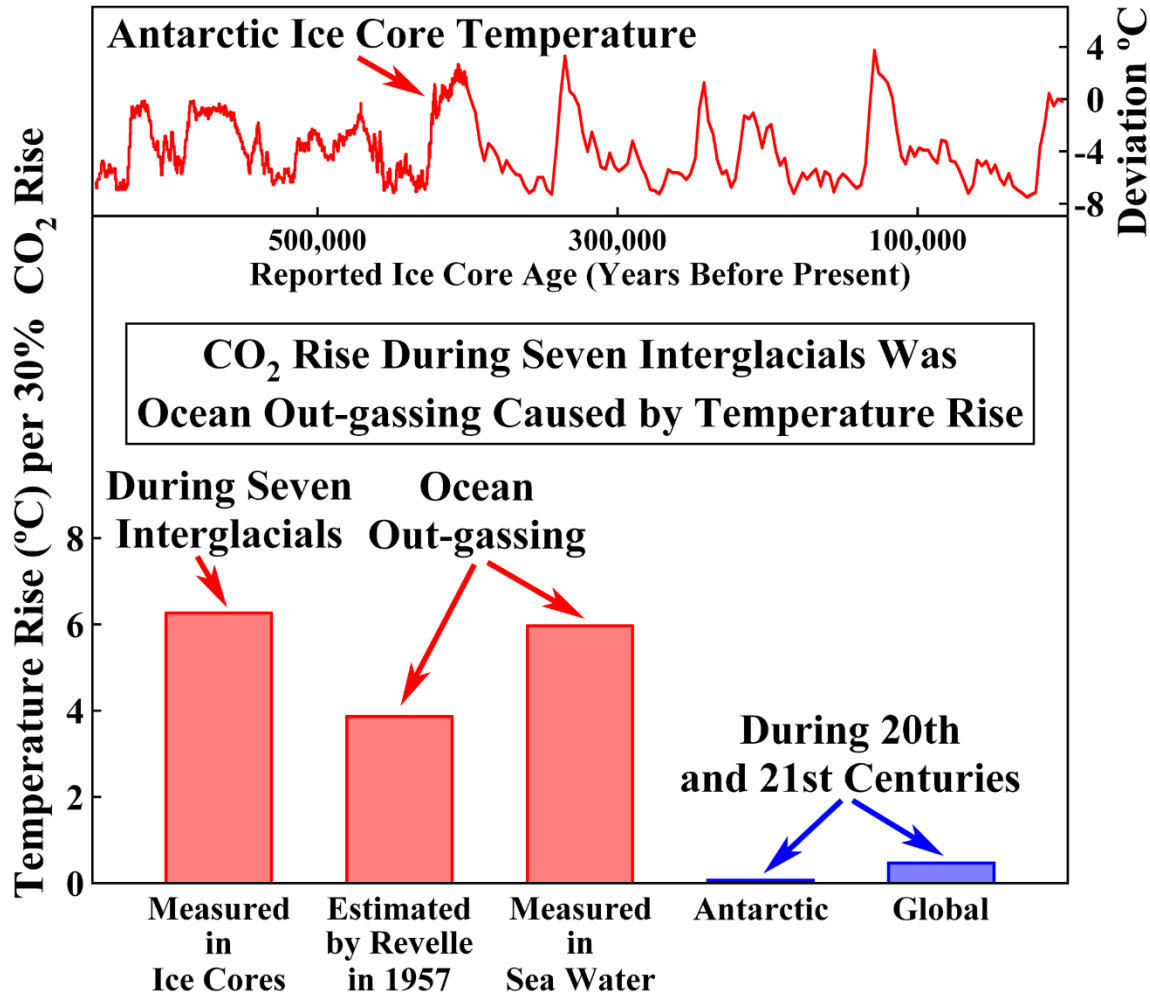


Figure 16: Temperature rise versus CO<sub>2</sub> rise from seven ice-core measured interglacial periods (63-65); from calculations (69) and measurements (70) of sea water out-gassing; and as measured during the 20th and 21st centuries rises through (10,72). The interglacial temperature increases caused the CO<sub>2</sub> release of ocean CO<sub>2</sub>. The CO<sub>2</sub> rises did not cause the temperature rises.

In addition to the agreement between the out-gassing estimates and measurements, this conclusion is also verified by the small temperature rise during the 20th and 21st centuries. If the CO<sub>2</sub> versus temperature correlation during the seven interglacials had been caused by CO<sub>2</sub> green house warming, then the temperature rise per CO<sub>2</sub> rise would have been as high during the 20th and 21st centuries as it was during the seven interglacial periods.

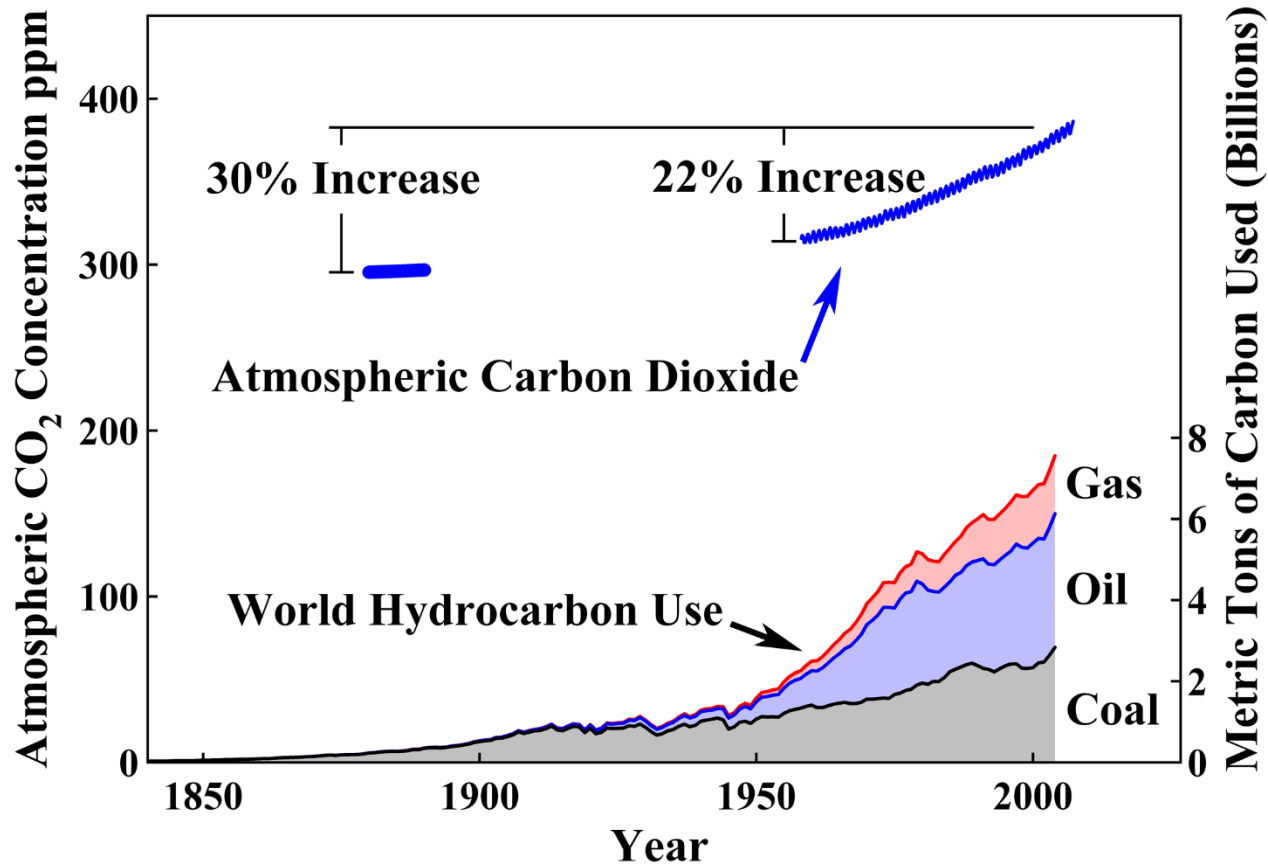


Figure 17: Atmospheric CO<sub>2</sub> concentrations in parts per million by volume, ppm, measured spectrophotometrically at Mauna Loa, Hawaii, between 1958 and 2007. These measurements agree well with those at other locations (71). Data before 1958 are from ice cores and chemical analyses, which have substantial experimental uncertainties. We have used 295 ppm for the period 1880 to 1890, which is an average of the available estimates. About 0.6 Gt C of CO<sub>2</sub> is produced annually by human respiration and of ten leads to concentrations exceeding 1,000 ppm in public buildings. Atmospheric CO<sub>2</sub> has increased 22% since 1958 and about 30% since 1880.

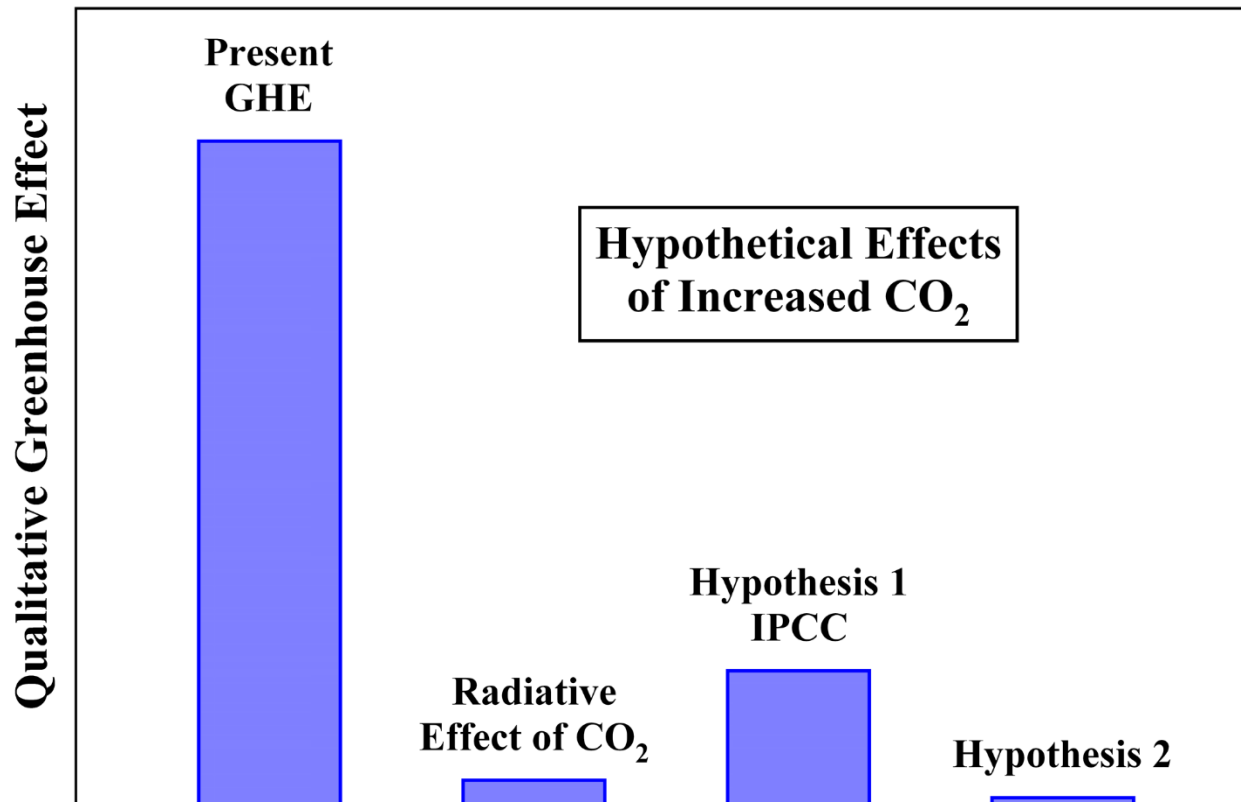


Figure 18: Qualitative illustration of green house warming. Present GHE is the current green house effect from all atmospheric phenomena. "Radiative effect of CO<sub>2</sub>" is the added greenhouse radiative effect from doubling CO<sub>2</sub> without consideration of other atmospheric components. "Hypothesis 1 IPCC" is the hypothetical amplification effect assumed by IPCC, "Hypothesis 2" is the hypothetical moderation effect.

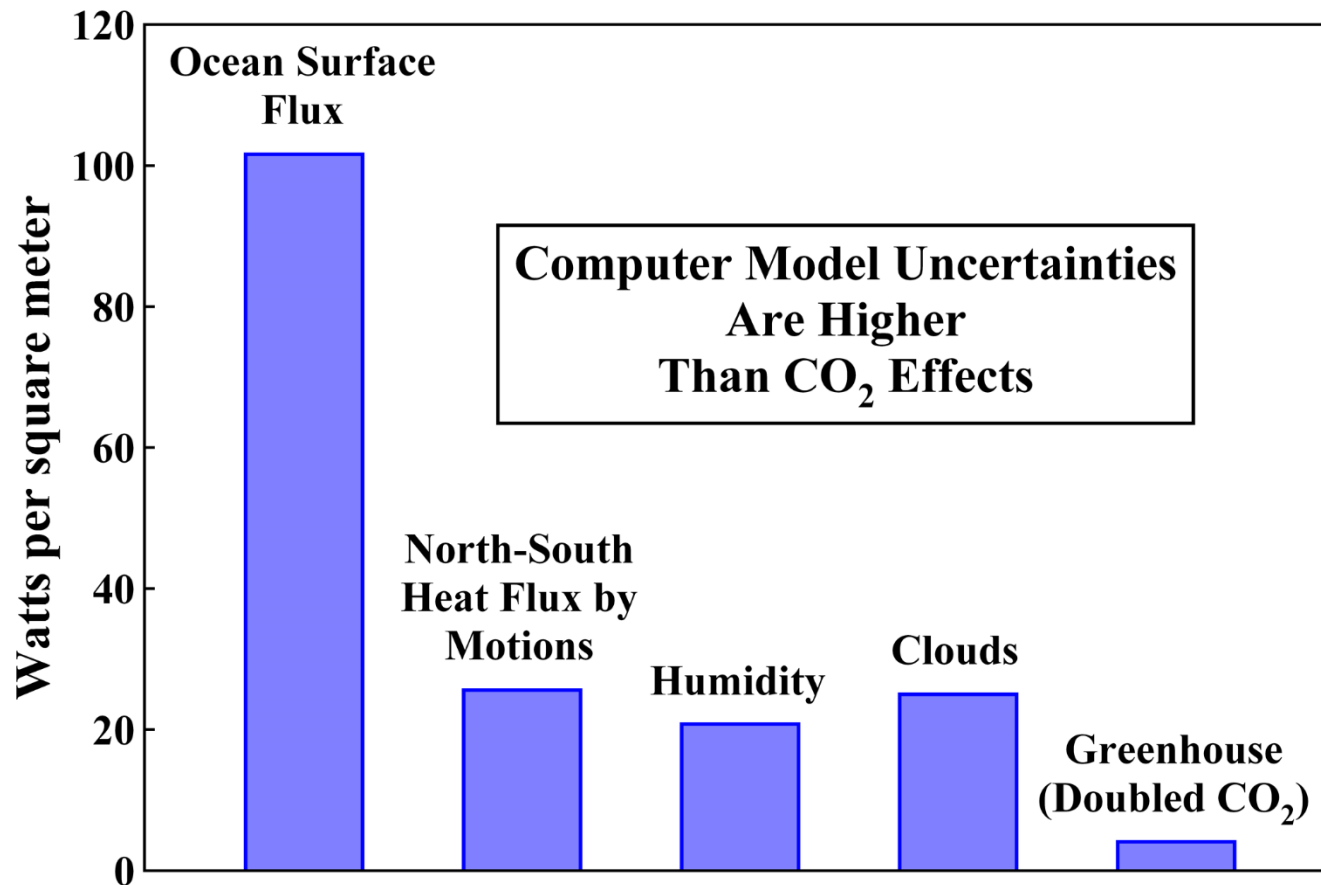


Figure 19: The radiative greenhouse effect of doubling the concentration of (right bar) as compared with four of the uncertainties in the atmospheric CO<sub>2</sub> computer climate models (87,93).

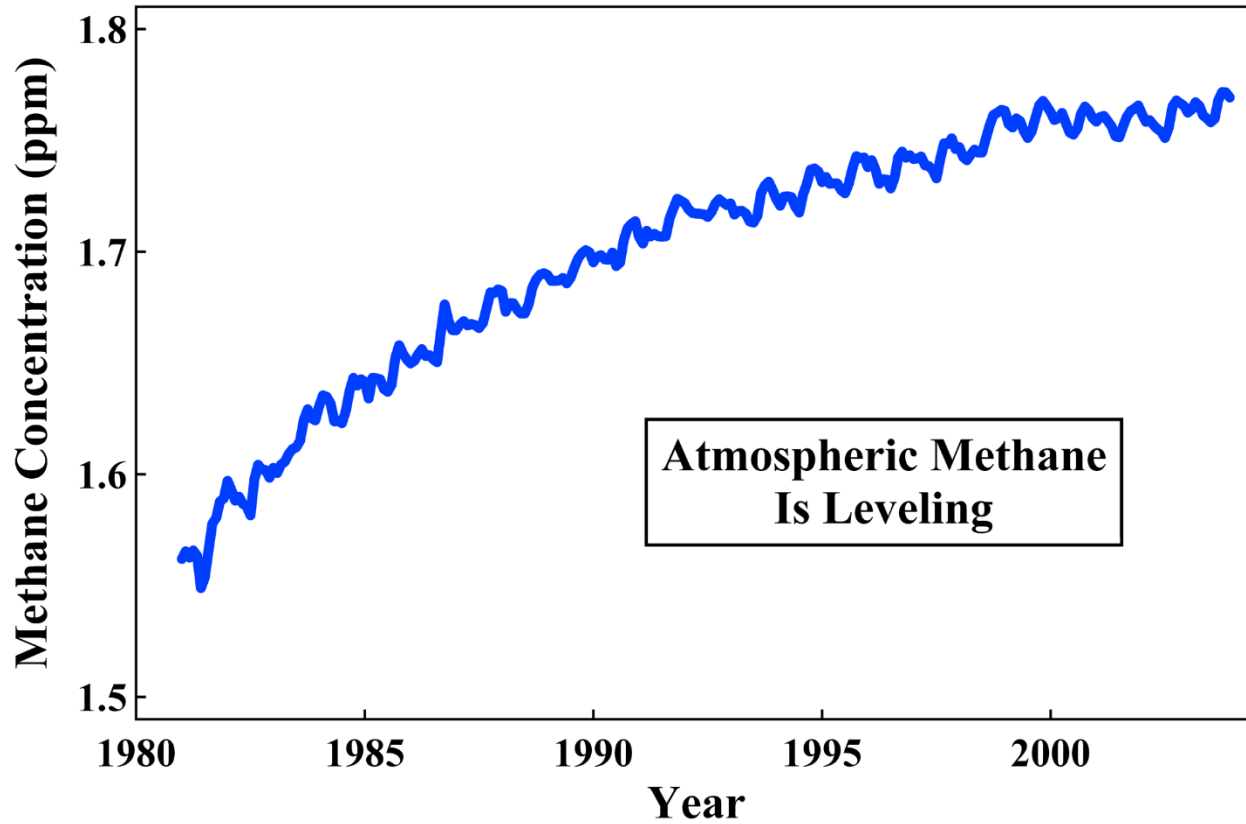


Figure 20: Global atmospheric methane concentration in parts per million between 1982 and 2004 (94).

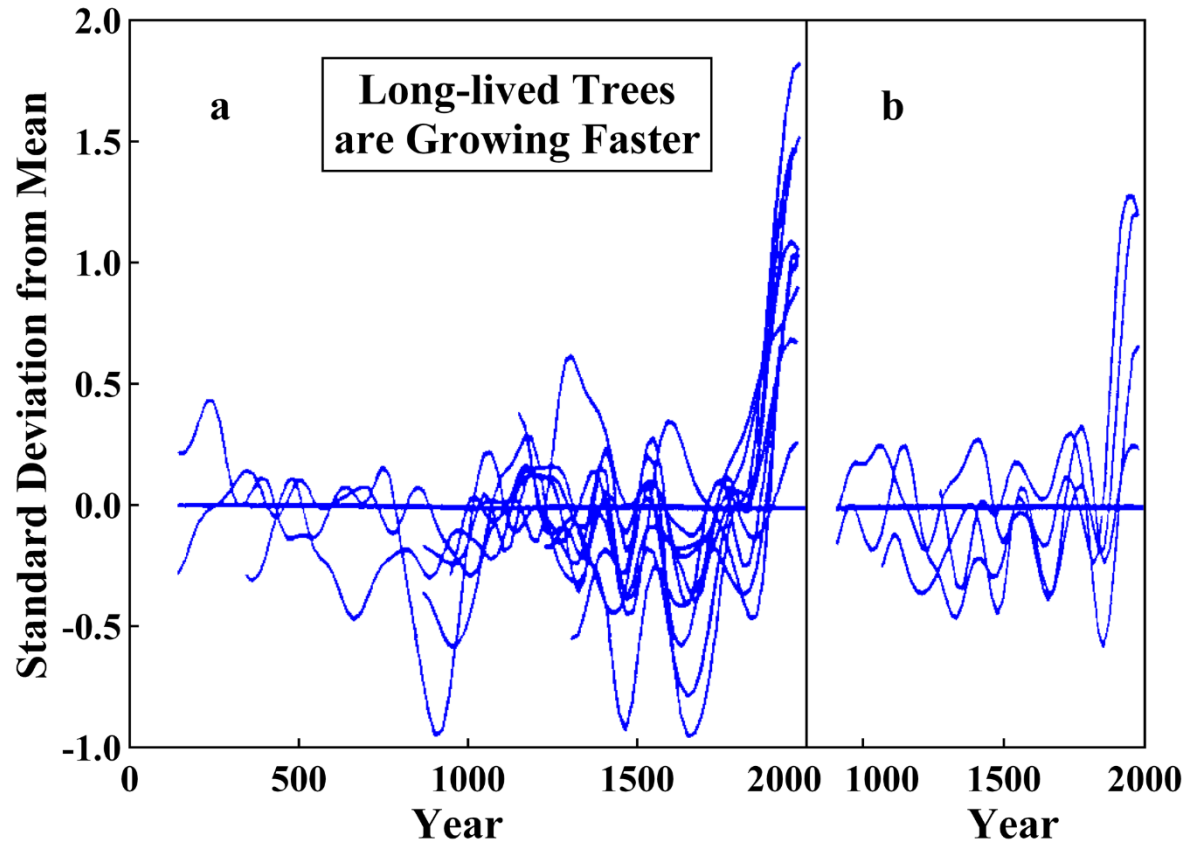


Figure 21: Standard deviation from the mean of tree ring widths for (a) bristlecone pine, limber pine, and fox tail pine in the Great Basin of California, Nevada, and Arizona and (b) bristlecone pine in Colorado (110). Tree ring widths were averaged in 20-year segments and then normalized so that the means of prior tree growth were zero. The deviations from the means are shown in units of standard deviations of those means.

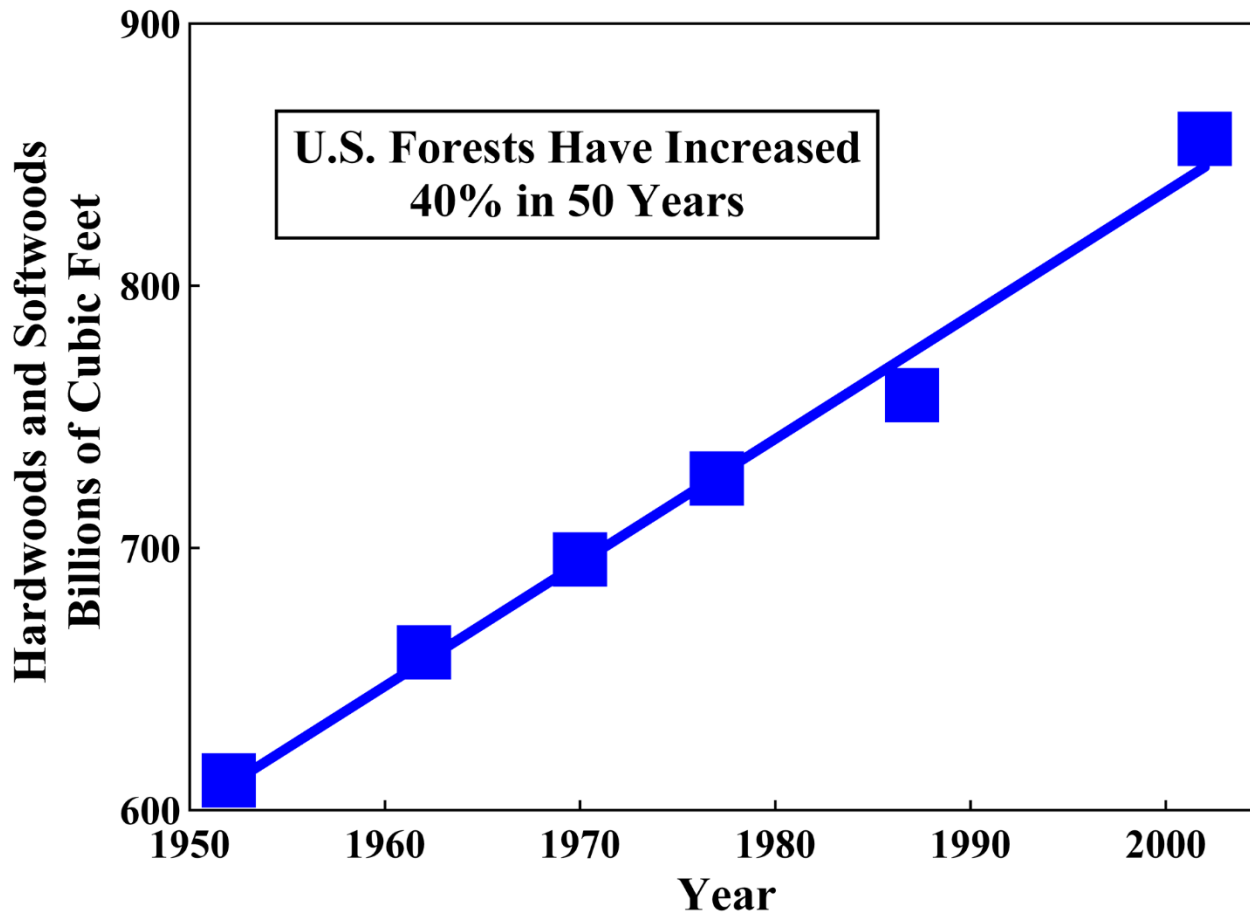


Figure 22: Inventories of standing hardwood and softwood timber in the, *United States compiled in Forest Resources of the United States 2002*, U.S. Department of Agriculture Forest Service (111,112). The linear trend cited in 1998 (1) with an increase of 30% has continued. The increase is now 40%. The amount of U.S. timber is rising almost 1% per year.

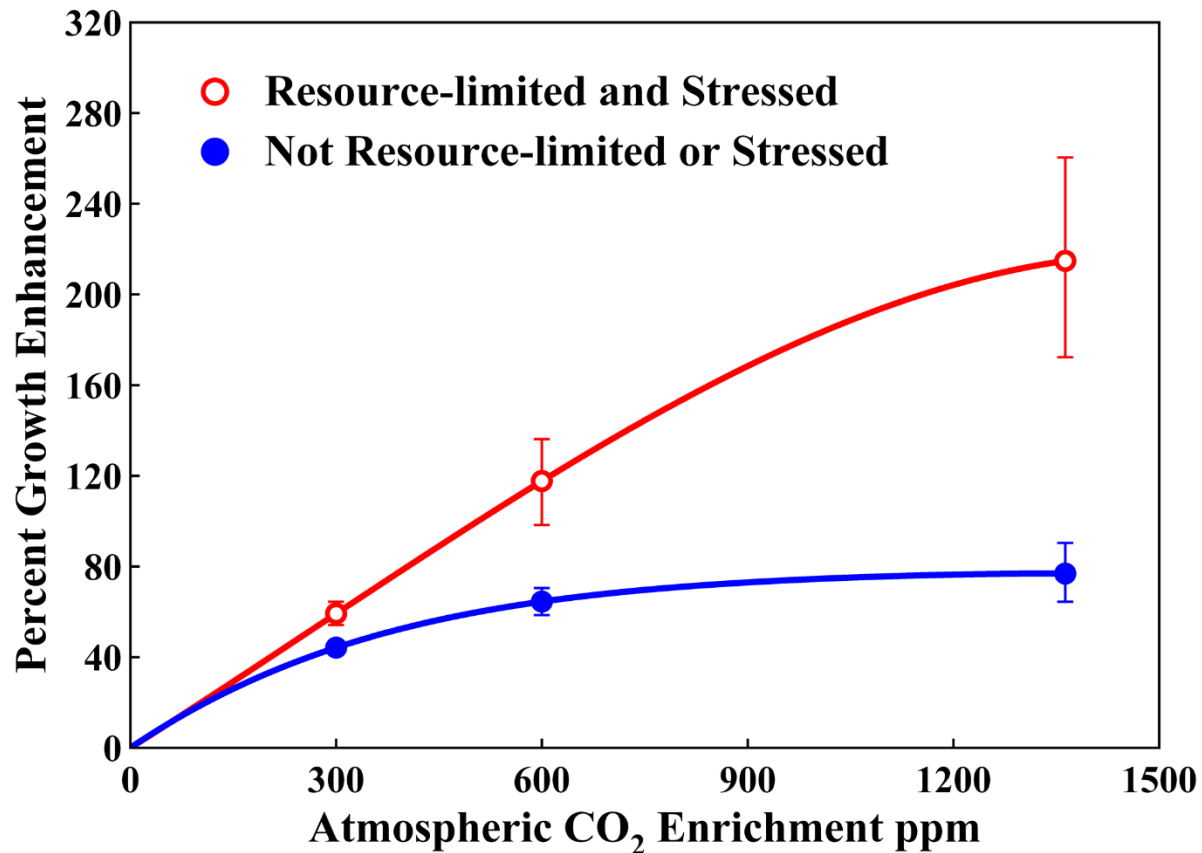


Figure 23: Summary data from 279 published experiments in which plants of all types were grown under paired stressed (open red circles) and unstressed (closed blue circles) conditions (114). There were 208, 50, and 21 sets at 300, 600, and an average of about 1350 ppm CO<sub>2</sub>, respectively. The plant mixture in the 279 studies was slightly biased toward plant types that respond less to CO<sub>2</sub> fertilization than does the actual global mixture. Therefore, the figure underestimates the expected global response. CO<sub>2</sub> enrichment also allows plants to grow in drier regions, further increasing the response.

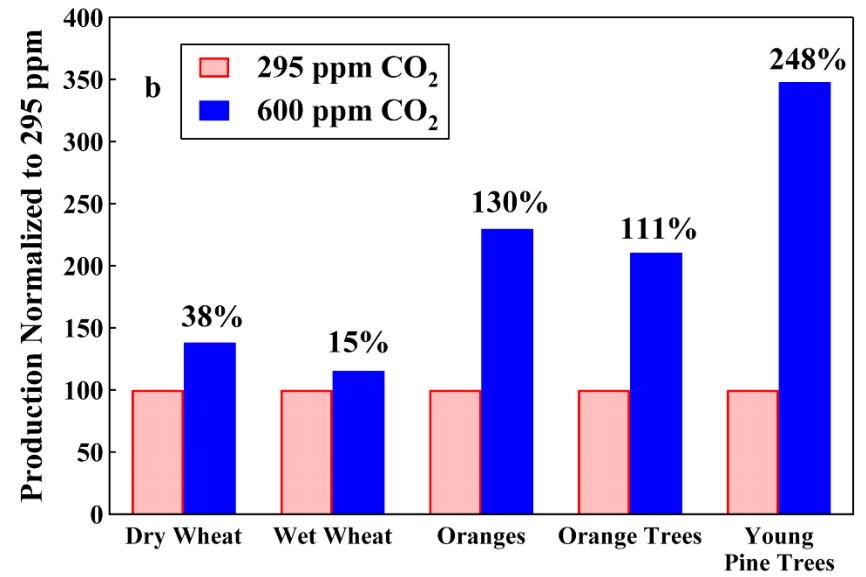
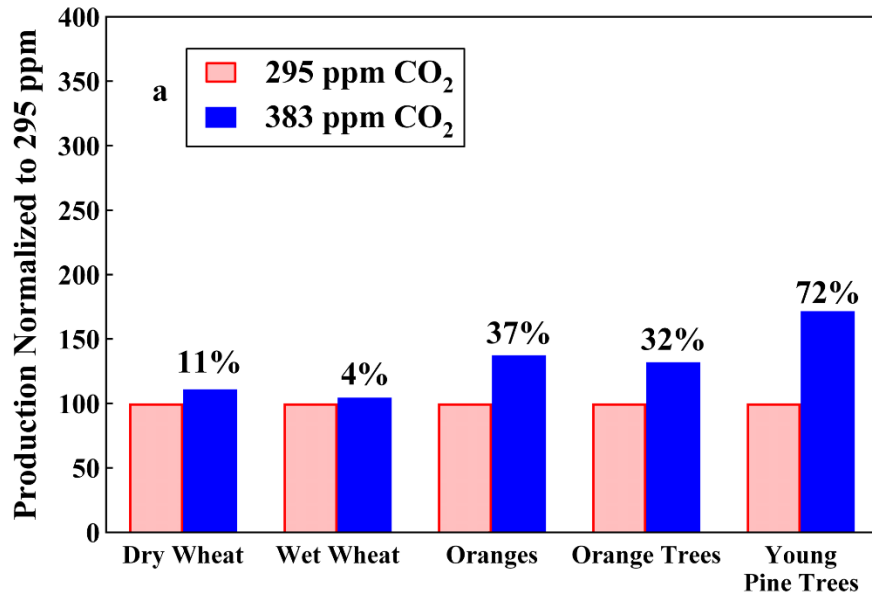


Figure 24: Calculated (1,2) growth rate enhancement of wheat, young orange trees, and very young pine trees already taking place as a result of atmospheric enrichment by CO<sub>2</sub> at from 1885 to 2007 (a), and expected as result of atmospheric enrichment by CO<sub>2</sub> to a level of 600 ppm (b).

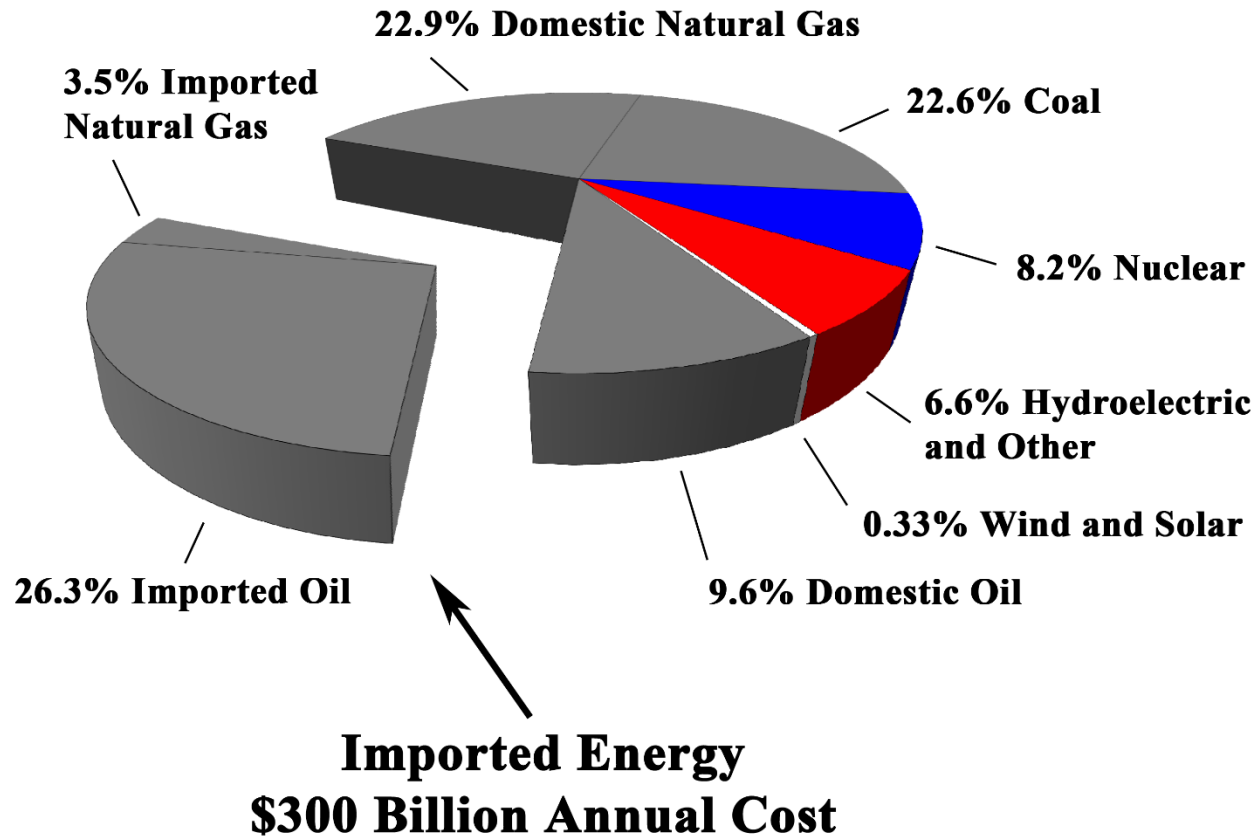


Figure 25: In 2006, the United States obtained 84.9% of its energy from hydrocarbons, 8.2% from nuclear fuels, 2.9% from hydroelectric dams, 2.1% from wood, 0.8% from biofuels, 0.4% from waste, 0.3% from geothermal, and 0.3% from wind and solar radiation. The U.S. uses 21 million barrels of oil per day 27% from OPEC, 17% from Canada and Mexico, 16% from others, and 40% produced in the U.S. (95). The cost of imported oil and gas at \$60 per barrel and \$7 per 1,000 ft<sup>3</sup> in 2007 is about \$300 billion per year.

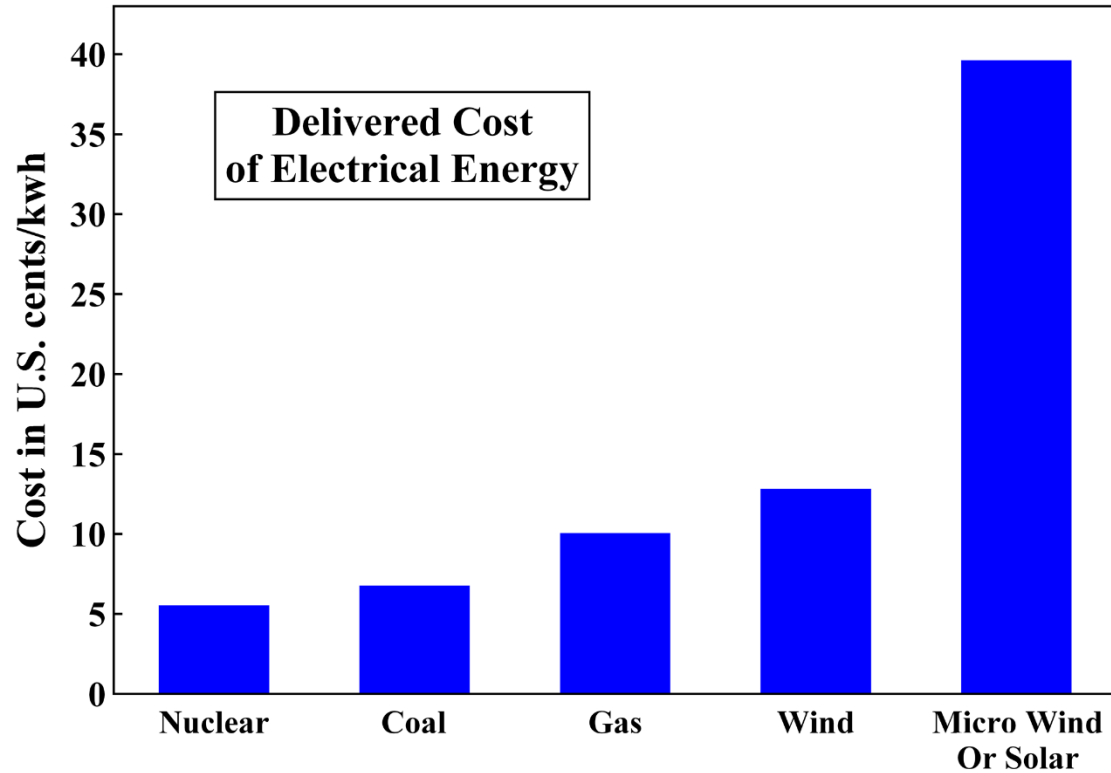


Figure 26: Delivered cost per kilowatt hour of electrical energy in Great Britain in 2006, without CO<sub>2</sub> controls (126). These estimates include all capital and operational expenses for a period of 50 years. Micro wind or solar are units installed for individual homes.

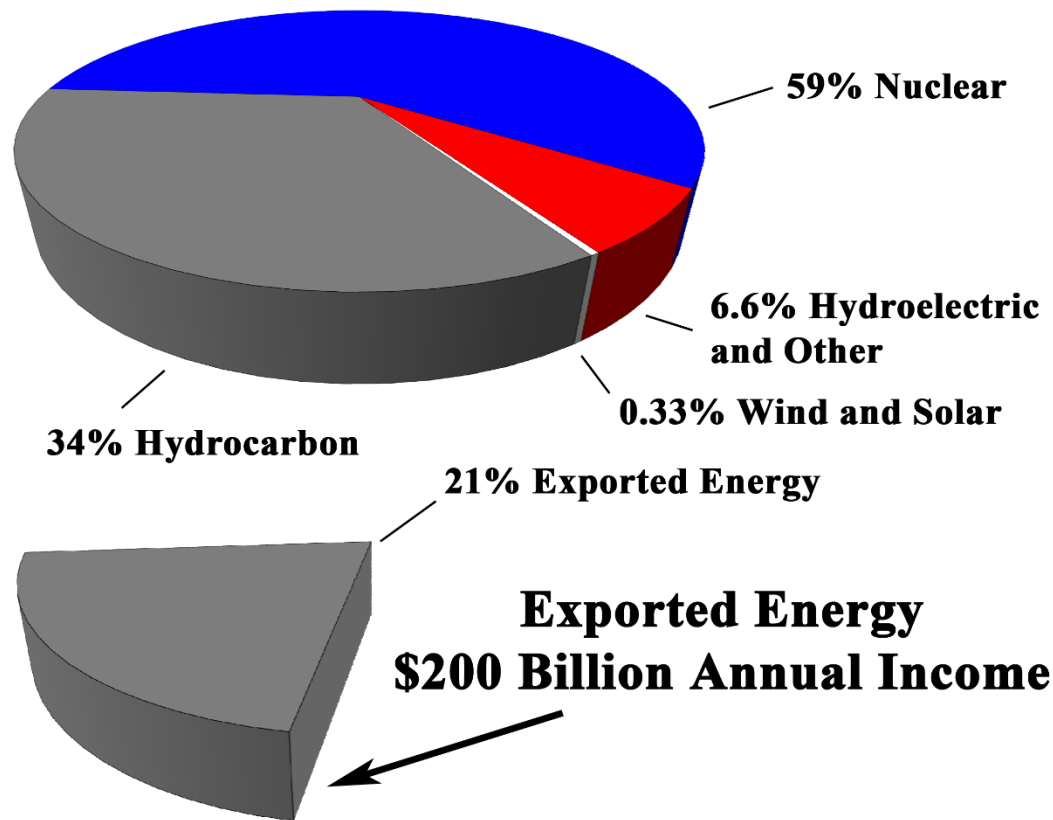


Figure 27: Construction of one Palo Verde installation with 10 reactors in each of the 50 states. Energy trade deficit is reversed by \$500 billion per year, resulting in a \$200 billion annual surplus. Currently, this solution is not possible owing to misguided government policies, regulations, and taxation and to legal maneuvers available to anti-nuclear activists. These impediments should be legislatively repealed.